AN ESTIMATION PROCEDURE FOR *J* AND CTOD FRACTURE PARAMETERS IN SQUARE GROOVE WELDS WITH CENTER CRACK

Gustavo H. B. Donato, gustavo.donato@poli.usp.br
Claudio Ruggieri, claudio.ruggieri@poli.usp.br
Department of Naval Architecture and Ocean Engineering, PNV-EPUSP
University of São Paulo, São Paulo, SP 05508−900, Brazil

Abstract *– This work presents an exploratory development of J and CTOD estimation procedures for welded fracture specimens under bending based upon plastic eta factors and plastic rotation factors. The techniques considered include: i) estimating J and CTOD from plastic work and ii) estimating CTOD from the plastic rotational factor. The primary objective is to gain additional understanding on the effect of weld strength mismatch on estimation techniques to determine J and CTOD fracture parameters for a wide range of a/W-ratios and mismatch levels. Very detailed non-linear finite element analyses for plane-strain models of SE(B) fracture specimens with center cracked, square groove welds provide the evolution of load with increased load-line displacement and crack mouth opening displacement which are required for the estimation procedure. The results show that levels of weld strength mismatch within the range* $\pm$ *20% mismatch do not affect significantly J and CTOD estimation expressions applicable to homogeneous materials, particularly for deeply cracked fracture specimens. The present analyses, when taken together with previous studies, provide a fairly extensive body of results which serve to determine parameters J and CTOD for different materials using bend specimens with varying geometries and mismatch levels.*

Keywords*: structural integrity, J-integral, CTOD, weldments, strength mismatch, SE(B) specimens*

1. INTRODUCTION

Structural integrity assessments of steel weldments (weld metal and heat affected zone – HAZ) remain a key issue for the safety analyses of critical welded structures, including pressure vessels, piping systems and storage tanks. Experimental observations consistently reveal the occurrence of crack-like defects in the welded region which are either planar (e.g., hot or cold cracking, lack of penetration, undercut) or volumetric (e.g., porosity and entrapped slag). To address the potential deleterious effects of such defects on the structural integrity, many codes and current fabrication practices require the use of weldments with weld metal strength higher than the base metal strength; a condition referred to as overmatching. An evident benefit of weld overmatching involves the capability to promote gross section yielding of the base plate due to the higher yield stress of the weld metal thereby shielding the welded region. Moreover, overmatch welds cause large plastic deformation into the lower strength base plate where the fracture toughness is presumably higher which also increases the load carrying capacity of the welded joint.

Fracture mechanics based approaches for structural components, including welded structures, rely upon the notion that a single parameter which defines the crack driving force characterizes the fracture resistance of the material (Hutchinson, 1983; Zerbst *et al.*, 2000; Anderson, 2005). These approaches allow the severity of crack-like defects to be related to the operating conditions in terms of a critical applied load or critical crack size. In particular, assessments of cleavage fracture for ferritic steels in the ductile-to-brittle transition (DBT) region are based on the one-parameter elastic-plastic characterization of macroscopic loading, most commonly the *J*-integral or the Crack Tip Opening Displacement (CTOD, δ), and their corresponding macroscopic measures of cleavage fracture toughness (J_c or δ_c). Several flaw assessment procedures make extensive use of these toughness parameter obtained from conventional fracture specimens to analyze the significance of defects in terms of assessments of structural integrity (SINTAP, 1999; API 579, 2000; BS7910, 1999).

Current standardized techniques, such as BS 7448 (1991), ASTM 1290 (1993) and ASTM 1820 (1996), to measure cleavage fracture resistance of structural steels routinely employ three-point bend SE(B) and compact tension C(T) specimens containing deep, through cracks ($a/W \geq 0.5$). Within these methodologies, evaluation of parameters *J* and CTOD derives from estimation formulas based upon laboratory measurements of load-displacement records. However, these testing procedures employ *J* and CTOD estimation expressions which are mainly applicable to homogeneous materials and, conse-

quently, do not incorporate the potentially strong effects of weld strength mismatch on the crack tip driving forces. Consequently, accurate estimation formulas for J and CTOD toughness parameters which are applicable to welded fracture specimens remains essential for more refined defect assessment procedures capable of including effects of weld strength mismatch on fracture toughness.

This work presents an exploratory development of J and CTOD estimation procedures for welded bend specimens based upon plastic *eta* factors and plastic rotation factors. The techniques considered include: i) estimating J and CTOD from plastic work and ii) estimating CTOD from the plastic rotational factor. The primary objective is to gain additional understanding on the effect of weld strength mismatch on estimation techniques to determine J and CTOD fracture parameters for a wide range of a/W-ratios and mismatch levels. Very detailed non-linear finite element analyses for plane-strain models of SE(B) fracture specimens with center cracked, square groove welds provide the evolution of load with increased load-line displacement and crack mouth opening displacement which are required for the estimation procedure. The results show that levels of weld strength mismatch within the range $\pm 20\%$ mismatch do not affect significantly J and CTOD estimation expressions applicable to homogeneous materials, particularly for deeply cracked fracture specimens. The present analyses, when taken together with previous studies, provide a fairly extensive body of results which serve to determine parameters J and CTOD for different materials using bend specimens with varying geometries and mismatch levels.

2. *J* AND CTOD ESTIMATION PROCEDURE

2.1 Eta Method

Evaluation of the J-integral from laboratory measurements of load-displacement records is most often accomplished by considering the elastic and plastic contributions to the strain energy for a cracked body under Mode I deformation (Anderson, 2005) as follows

$$J = J_{el} + J_{pl} \tag{1}$$

where the elastic component, J_{el}, is given by

$$J_{el} = \frac{K_I^2}{E'} \quad . \tag{2}$$

Here, the elastic stress intensity factor, K_I, is defined for a SE(B) specimen as

$$K = \frac{PS}{BW^{3/2}} \mathfrak{F}(a/W) \tag{3}$$

where P is the applied load, B is the specimen thickness, W is the specimen width, S is the specimen span and $\mathfrak{F}(a/W)$ defines a nondimensional stress intensity factor given by (Anderson, 2005)

$$\mathfrak{F}(a/W) = g_1\left(\frac{a}{W}\right)\left[1.99 - \frac{a}{W}\left(1 - \frac{a}{W}\right)g_2\left(\frac{a}{W}\right)\right] \tag{4}$$

and

$$g_1\left(\frac{a}{W}\right) = \frac{3\left(\frac{a}{W}\right)^{1/2}}{2\left(1 + 2\frac{a}{W}\right)\left(1 - \frac{a}{W}\right)^{3/2}} \tag{5}$$

$$g_2\left(\frac{a}{W}\right) = 2.15 - 3.93\left(\frac{a}{W}\right) + 2.7\left(\frac{a}{W}\right)^2 \quad . \tag{6}$$

The plastic component, J_{pl}, is conveniently evaluated from the plastic area under the load-displacement curve as

$$J_{pl} = \frac{\eta_J A_{pl}}{B(W - a)} \tag{7}$$

where A_{pl} is the plastic area under the load-displacement curve and factor η_J represents a nondimensional parameter which describes the effect of plastic strain energy on the applied J (Sumpter and Turner, 1976; Rice *et al.*, 1973). The previous definition for J_{pl} derives from the assumption of nonlinear elastic material response thereby providing a deformation plasticity quantity. Figure 1(a) illustrates the procedure to determine the plastic area to calculate J from a typical load-displacement curve. It should be noted that A_{pl} (and consequently η_J) can be defined in terms of load-load line displacement (LLD or Δ) data or load-crack mouth opening displacement (CMOD or V) data. While factors η_J derived from each curve posses a different character they serve equally as a means to determine J_{pl} from laboratory measurements of load-displacement records; here, these quantities are denoted η_J^{LLD} and η_J^{CMOD}.

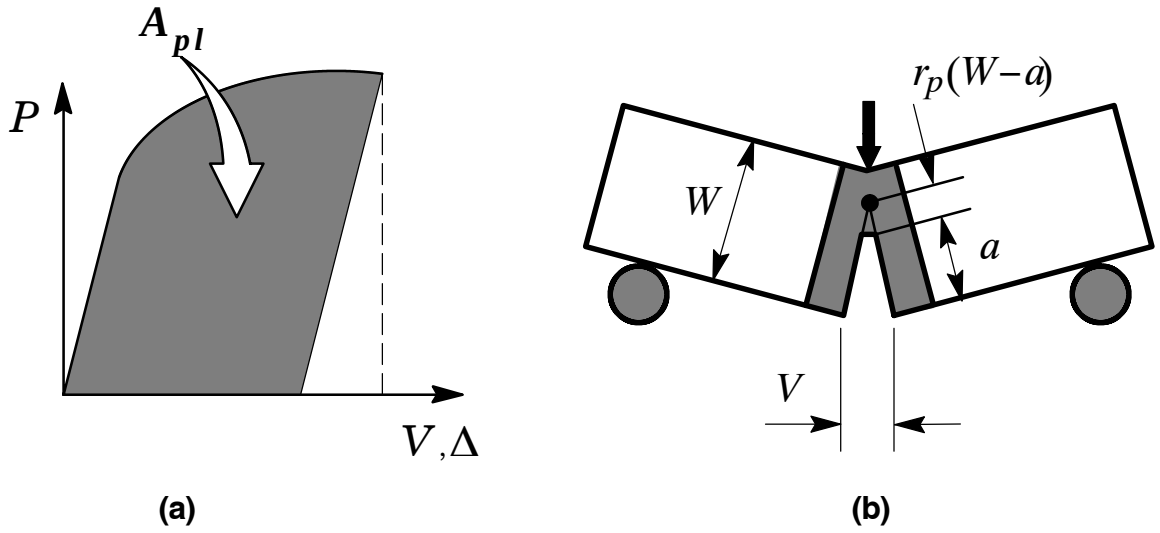

Figure 1 *(a) Definition of the plastic area under the load-displacement (CMOD or LLD) curve; (b) Plastic hinge model employed to estimate CTOD.*

Following the previous energy release rate interpretation of the J-integral and using the connection between J and δ (Anderson, 2005), a similar formulation also applies when the CTOD is adopted to characterize the material's fracture resistance. Experimental CTOD-values are then evaluated by

$$\delta = \delta_{el} + \delta_{pl} \tag{8}$$

where

$$\delta_{el} = \frac{K_I^2}{m\sigma_f E'} \tag{9}$$

and

$$\delta_{pl} = \frac{\eta_\delta A_{pl}}{B\sigma_f (W - a)} \quad . \tag{10}$$

where factor η_δ represents a nondimensional parameter which describes the effect of plastic strain energy on the applied CTOD. In the above expressions, parameter m represents a plastic constraint factor which is most often assigned a value of 2 in current standards (BS 7448, 1991; ASTM 1290, 1993) and σ_f denotes the flows stress defined as $\sigma_f = (\sigma_{ys} + \sigma_t)/2$ where σ_{ys} is the yield stress and σ_t is the (ultimate) tensile strength.

The previous development based upon the *eta*-factor retains strong contact with current standards to determine experimental J-values using common fracture specimens for homogeneous materials. Computation of *eta*-factors for fracture specimens made of heterogeneus materials, such as welded crack configurations, is relatively straightforward and derives from plane-strain analyses as described in the next sections. Further, generalization of the *eta*-methodology in estimation procedures for elastic-plastic fracture toughness (J, δ) involves two key benefits: 1) it provides a simpler and yet more accurate procedure to determine the CTOD and 2) it imposes no restrictions on flow properties (essentially yield stress and hard-

ening behavior) for the tested material. The following sections explore these issues and provide detailed analyses which yield *eta*-factors applicable to determine J and CTOD in SE(B) specimens with a wide range of crack sizes, weld groove width and mismatch levels.

2.2 Plastic Hinge Model

Current standards to estimate the crack tip opening displacement from measured load-CMOD record for homogeneous fracture specimens, such as BS 7448 (1991) and ASTM 1290 (1993), also adopt separation of the CTOD parameter into its elastic and plastic components as given by the previous Eq. (8). Within these methodologies, the plastic component of CTOD, defined by δ_{pl}, is derived from considering that the test specimen rotates about a plastic hinge located in the crack ligament. The procedure is also applicable to a square groove weld such as illustrated schematically in Fig. 1(b).

By assuming straight crack flanks and using a similar triangle construction, δ_{pl} is simply related to the plastic displacement at the crack mouth, V_{pl}, through the expression

$$\delta_{pl} = \frac{r_p(W - a)V_{pl}}{r_p(W - a) + a + z} \tag{11}$$

where z is the knife edge height ($z = 0$ if the clip gage is attached directly in the specimen – see BS 7448 (1991) and ASTM 1290 (1993)) and r_p is the plastic rotational factor which defines the relative position of the (apparent) hinge point (see Fig. 1(b)). For deeply cracked, homogeneous SE(B) specimens, r_p takes on the value of 0.44 in ASTM 1290 (1993) and 0.4 in BS 7448 (1991).

3. NUMERICAL PROCEDURES

3.1 Finite Element Models

Detailed finite element analyses are performed on plane-strain models for a wide range of 1-T SE(B) specimens ($B = 25.4$ mm and conventional geometry with $W = 2B$ and $S/W = 4$) having a center cracked, square groove weld with different groove width and weld strength mismatch. The analysis matrix includes specimens with $a/W = 0.1$, 0.15, 0.2, 0.25, 0.3, 0.5 and 0.7 and $h = 5$ and 20 mm. Here, a is the crack size specimen, W is the specimen width, S is the specimen span and h is the weld groove width. Figure 2(a) shows the geometry and specimen dimensions for the analyzed crack configurations.

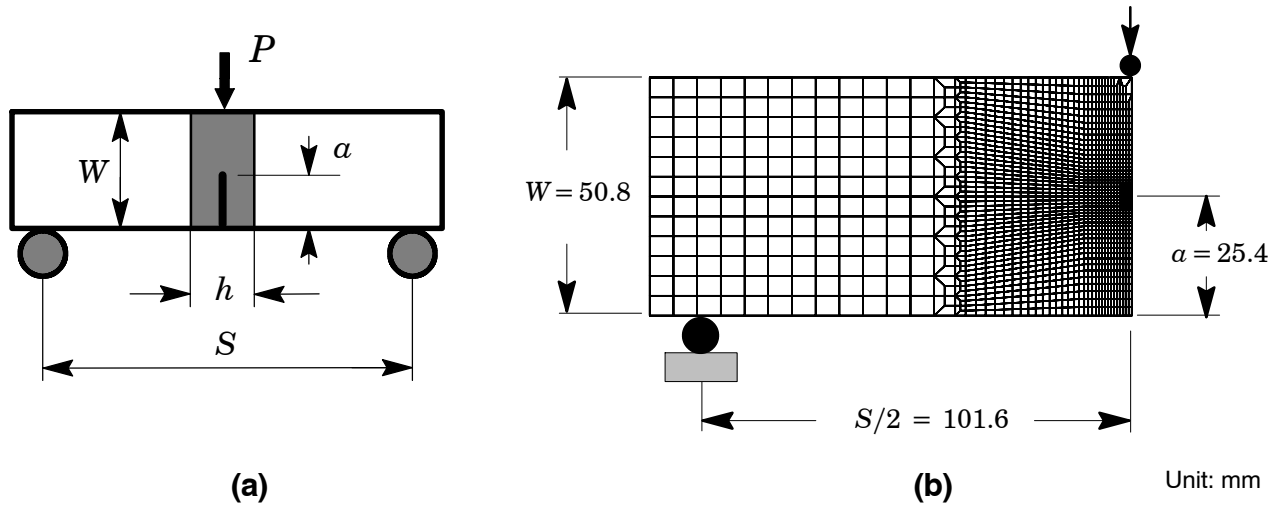

Figure 2 *(a) Geometry for analyzed SE(B) fracture specimens with a center crack, square groove weld; (b) Finite element model used in plane-strain analyses of the deeply cracked SE(B) specimen with a/W = 0.5.*

Figure 2(b) shows the finite element model constructed for the plane-strain analyses of the deeply-cracked SE(B) specimen with $a/W = 0.5$ and a center-cracked, square-grooved weld. The weld fracture specimen is modelled as bimaterial with no transition region, *i.e.*, the heat affected zone (HAZ) is not considered. All other crack models have very similar features. A conventional mesh configuration having a focused ring of elements surrounding the crack front is used with a small key-hole at the crack tip; the radius of the key-hole, ϱ_0, is 2.5μm (0.0025 mm). Symmetry conditions permit modeling of only one-half of the specimen with appropriate constraints imposed on the remaining ligament. The half-symmetric model has one thickness layer of 1241 8-node, 3-D elements (2678 nodes) with plane-strain constraints imposed ($w = 0$) on each node.

These finite element models are loaded by displacement increments imposed on the loading points to enhance numerical convergence.

3.2 Computational Procedures

The finite element code WARP3D (Koppenhoefer *et al.*, 1994) provides the numerical solutions for the plane-strain analyses reported here. The code incorporates both a Mises (J_2) constitutive model in both small-strain and finite-strain framework. Evaluation of the J-integral derives from a domain integral procedure (Moran and Shih, 1987) which yields J-values in excellent agreement with estimation schemes based upon *eta*-factors for deformation plasticity (Anderson, 2005) while, at the same time, retaining strong path independence for domains defined outside the highly strained material near the crack tip. Evaluation of the numerical value of CTOD follows the 90° procedure (Anderson, 2005) to the deformed crack flanks.

3.3 Material Laws

Evaluation of factor η requires nonlinear finite element solutions which include the effects of plastic work on J (δ) and the load-displacement response. These analyses utilize an elastic-plastic constitutive model with J_2 flow theory and conventional Mises plasticity in small geometry change (SGC) setting. The numerical solutions employ a simple power-hardening model to characterize the uniaxial true stress-logarithmic strain in the form

$$\frac{\epsilon}{\epsilon_0} = \frac{\bar{\sigma}}{\sigma_0} \quad \epsilon \le \epsilon_0 \; ; \qquad \frac{\epsilon}{\epsilon_0} = \left(\frac{\bar{\sigma}}{\sigma_0}\right)^n \quad \epsilon > \epsilon_0 \tag{12}$$

where σ_0 and ϵ_0 are the reference (yield) stress and strain, and n is the strain hardening exponent.

The finite element analyses consider material flow properties covering a wide range of strength mismatch: 80% undermatch, 20%, 50% and 100% overmatch. The welds are modelled as bimaterials (the heat affected zone , HAZ, is not considered in the present work) with the yield stress and hardening property of the base plate adopted as fixed in all analyses and assigned the following properties: $n = 10$ and $\sigma_0 = 412$ MPa. Table 1 provides the material properties utilized in the numerical analyses of the fracture specimens with square groove welds which also consider $E = 206$ GPa and $\nu = 0.3$. The strain hardening parameters for the weld metal are estimated from a simple correlation between the yield stress and hardening exponent applicable for typical structural steels: $n = 5$ and $E/\sigma_0 = 800$ (high hardening material), $n = 10$ and $E/\sigma_0 = 500$ (moderate hardening material), $n = 20$ and $E/\sigma_0 = 300$ (low hardening material). These ranges of properties also reflect the upward trend in yield stress with the decrease in strain hardening exponent characteristic of ferritic steels. The hardening exponents for the weld metal are given by linear interpolation of the previous adopted values for σ_0 and n.

Table 1 *Material properties adopted in the analyses of the weldments.*

Mismatch Level	Weld		Base Plate	
	σ_0 (MPa)	n	σ_0 (MPa)	n
20% Undermatch	330	7.3	412	10
20% Overmatch	494	12.8	412	10
50% Overmatch	618	17.4	412	10
100% Overmatch	824	25.5	412	10
Evenmatch	412	10	412	10

Evaluation of the plastic CTOD using the *eta*-method through Eq. (10) and the plastic hinge model through Eq. (11) requires especification of the tensile stress, σ_t, to compute the flow stress, σ_f. For each material property set, σ_t is estimated using the following relationship (Anderson, 2005)

$$\sigma_t = \sigma_{ys}\left[\frac{(500N)^N}{\exp(N)}\right] \quad . \tag{13}$$

where $N = 1/n$.

4. PLASTIC *ETA*-FACTORS

Evaluation of plastic η-factors for the analyzed crack configurations follows from solving Eqs. (7) and (10) upon computation of the plastic area, A_{pl} under the load-LLD or load-CMOD curve. A key question to resolve with the numerical proce-

dure lies in the choice of the deformation level (CMOD or LLD) at which A_{pl} (and consequently η) is evaluated. For very low deformation levels, the elastic component of the area under the load-deformation curve, A_{el}, has a magnitude which is comparable with the corresponding magnitude of the plastic component, A_{pl}, thereby affecting the computed η-value. Figure 3 displays the evolution of η_J^{CMOD} with increasing deformation (as measured by J) for the deeply cracked SE(B) specimen ($a/W = 0.5$) with 20% and 50% overmatch and groove size $h =$ 20 mm. The plastic η-factor varies strongly at low deformation levels but reaches a "plateau" when $A_{pl} \gg A_{el}$. Guided by numerical experiences, the η-value is then determined based upon the following procedure: 1) eliminate all η-values determined at low deformation levels and for which $A_{pl} \leq 0.1(A_{el} + A_{pl})$; 2) compute the η-value for the analyzed specimen as the average of the remaining η-values (which all lie on the plateau – see Fig. 3).

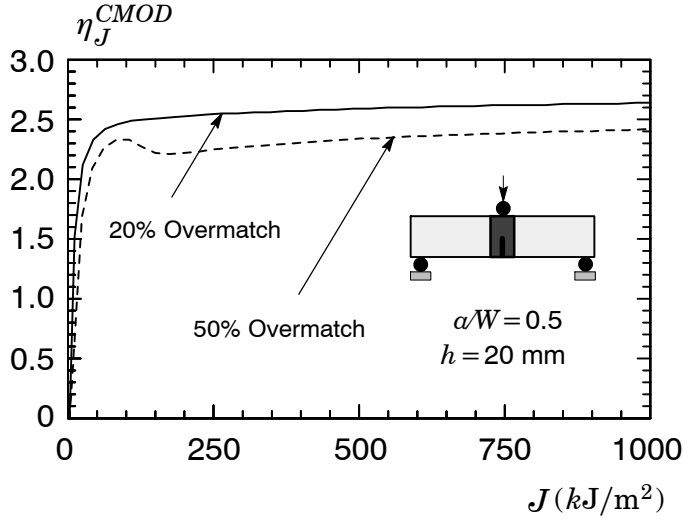

Figure 3 *Variation of factor η_J derived from CMOD with increased levels of J for the deeply cracked SE(B) specimen ($a/W = 0.5$) with 20% and 50% overmatch.*

Figures 4-6 provide the essential results from the plane-strain analyses needed to determine the elastic-plastic parameters J and CTOD for different weldment properties and specimen configurations. Figure 4 shows the variation of η_J^{LLD} with increased a/W-ratio and different mismatch levels with groove sizes $h = 5$ and 20 mm. The results displayed in this graph reveal that factor η_J derived from LLD exhibits very little sensitivity to mismatch level for the narrow groove size ($h = 5$ mm); in contrast, the effect of mismatch level on factor η_J for the groove size $h = 20$ mm is rather more pronounced. However, further examination of the results shown in the plot displayed in Fig. 4(b) reveals that η_J-values based on LLD for mismatch levels in the range $\pm 20\%$ mismatch follow closely the corresponding values for the evenmatch condition. Figure 5 provides the effect of mismatch level on η_J^{CMOD} with increased values of a/W. Here, the behavior of η_J^{CMOD} with varying levels of strength mismatch is similar to the previous results. While the strength mismatch does affect the values of factor η_J for the groove width $h = 20$ mm, the η_J^{CMOD}-values are similar to the evenmatch condition in the range $\pm 20\%$ mismatch, particularly for the 20% overmatch.

Figure 6 shows the variation of plastic *eta*-factors to determine the plastic component of CTOD, defined by η_δ^{CMOD}, with increased a/W-ratio and different mismatch levesl for groove sizes $h = 5$ and 20 mm. Compared to the previous results, a different picture now emerges as the effect of mismatch level is more pronounced for the narrow groove size ($h = 5$ mm). Because the value of the flow stress, σ_f, enters directly into the evaluation of factor η_δ^{CMOD} (recall Eq. (10)), the *relative* difference between the yield stress values for the weld metal and base plate plays a strong role on the evaluation of the plastic component of the CTOD, δ_{pl}, and, consquently, on η_δ^{CMOD}; this effect is more significant for narrow groove sizes as demonstrated by the results. However, for larger groove sizes this effect is much less pronounced; here, the η_δ-values based on CMOD for mismatch levels in the range $\pm 20\%$ are closer to the corresponding values for the evenmatch condition.

5. PLASTIC ROTATION FACTORS

The plastic rotation factor, r_p, is derived from evaluation of Eq. (11) for each analyzed SE(B) specimen configuration with varying mismatch levels. Since r_p depends on the position of the hinge point (see Fig. 1(b)), it may be anticipated that r_p will also depend on CMOD. Fig. 7 shows the variation of the plastic rotation factor with CMOD for the deeply cracked SE(B)

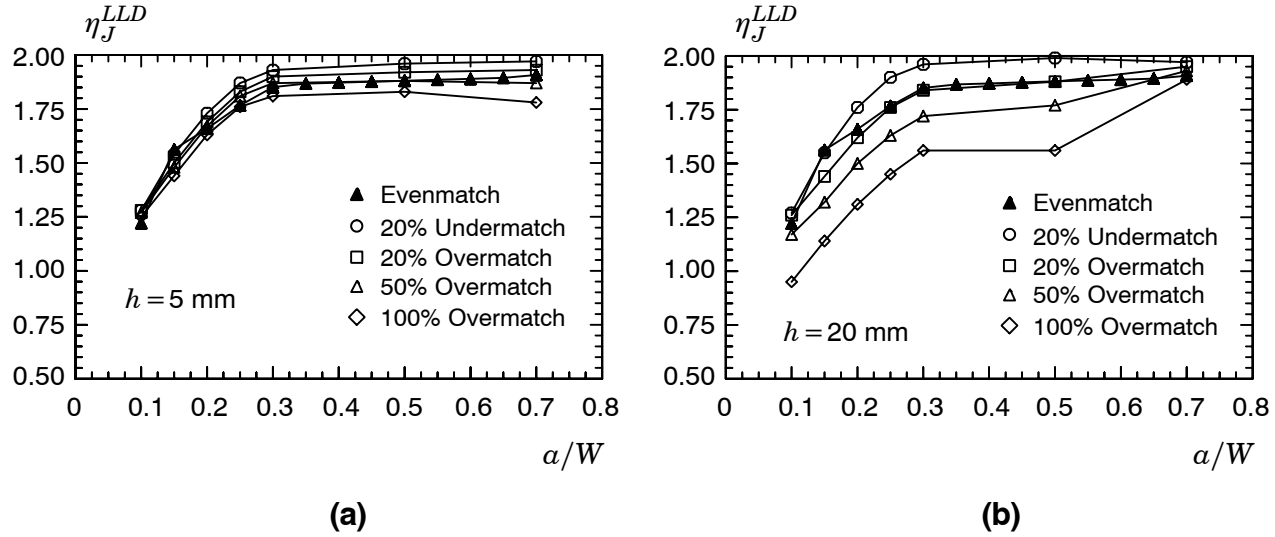

Figure 4 *Variation of plastic η_J derived from LLD with increased a/W-ratio and different mismatch levels for $h = 5$ and 20 mm groove sizes.*

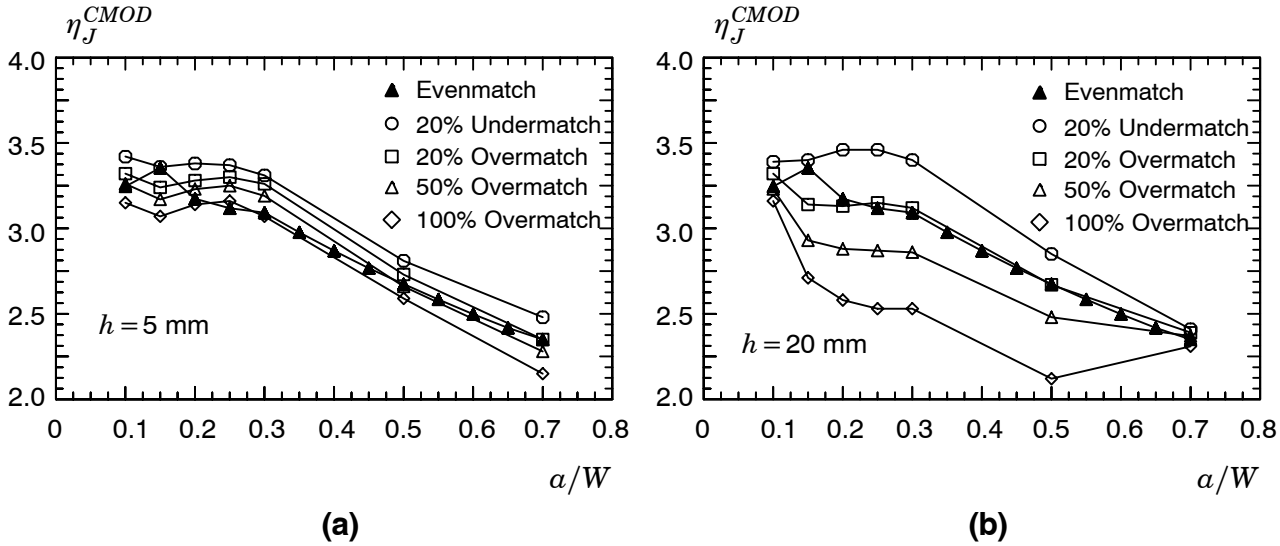

Figure 5 *Variation of plastic η_J derived from CMOD with increased a/W-ratio and different mismatch levels for $h = 5$ and 20 mm groove sizes.*

specimen ($a/W = 0.5$) with 20% and 50% overmatch and groove size $h = 20$ mm. The r_p-factor varies strongly for low values of CMOD for which the plastic component is small. In contrast, with increased values of CMOD, factor r_p does approach the ASTM value of 0.44 as indicated in the plot.

Figure 8 provides the variation of factor r_p with increased a/W-ratio for different mismatch levels. These r_p-factors represent the constant values which develop in the r_p *vs.* V plot for each specimen and mismatch level (see Fig. 7). For deeply cracked bend specimens ($a/W \gtrsim 0.4 \sim 0.45$), the r_p-values can be assumed essentially independent of crack size and mismatch level. For the shallow cracks, the r_p-values display more sensitivity to mismatch level, particularly for the groove size $h = 20$ mm. However, the effect of strength mismatch on the r_p-value is much less pronounced in the range $\pm 20\%$ mismatch as it follows closely the corresponding values for the evenmatch condition.

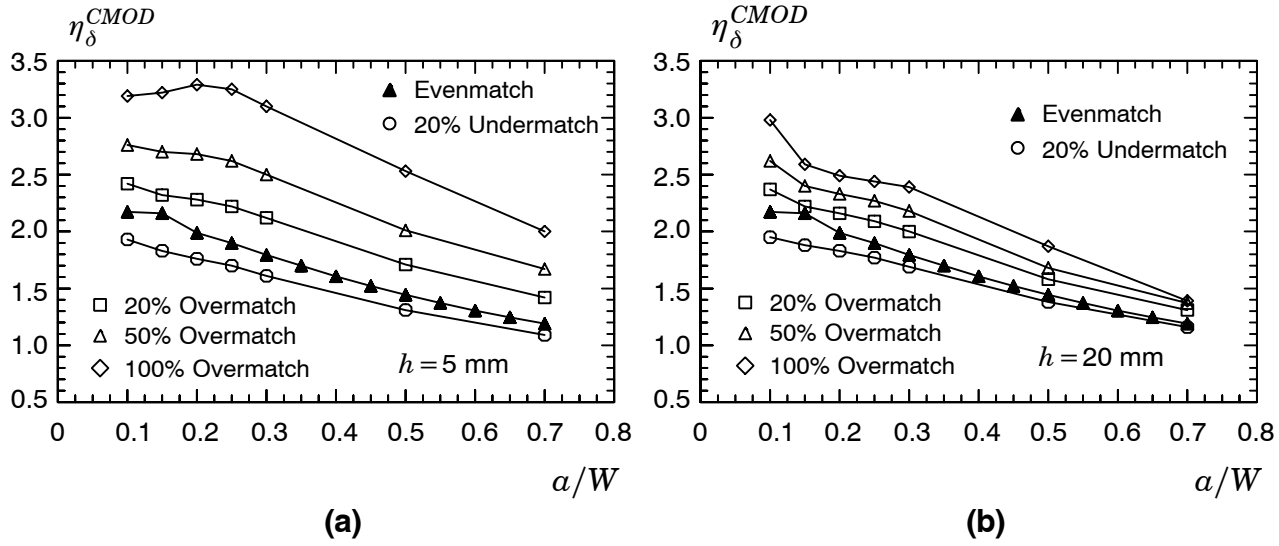

Figure 6 *Variation of plastic η_δ derived from CMOD with increased a/W-ratio and different mismatch levels for $h = 5$ and 20 mm groove sizes.*

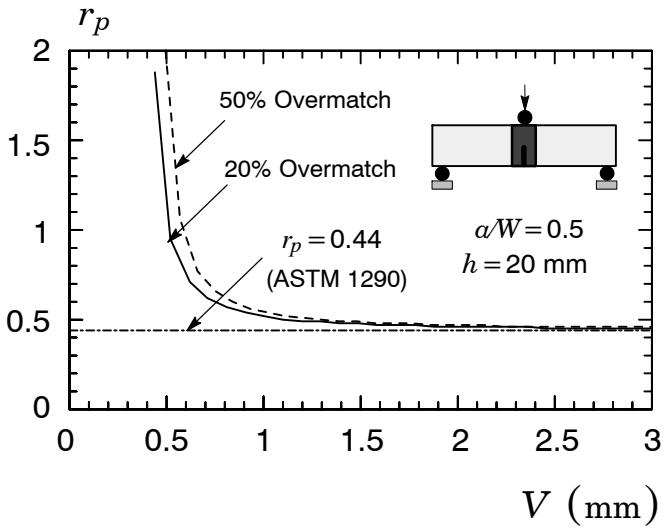

Figure 7 *Variation of plastic rotation factor, r_p, with increased levels of CMOD for the deeply cracked SE(B) specimen ($a/W = 0.5$) with 20% and 50% overmatch.*

6. MISMATCH EFFECTS ON THE *J*-INTEGRAL

This section examines the effect of weld strength mismatch on the crack-tip driving force as measured by the *J*-integral for a deep ($a/W = 0.5$) and shallow crack ($a/W = 0.2$) SE(B) specimen with a center-cracked, square-grooved weld (see Fig. 2). The primary objective is to assess the potential errors which arise from evaluating *J*-values using estimation formulas developed for homogeneous materials.

Figure 9 compares the *J*-values obtained from the analyses conducted for the mismatched crack configuration (refer to Table 1) and analyses conducted for an $h = 20$ mm grooved SE(B) specimen made of a homogeneous material having the weld metal properties corresponding to the mismatch condition (refer again to Table 1); this condition is referred to as "all weld metal" (AWM). To construct the plots displayed in Fig. 9, both *J*-values, hereafter denoted J_{Mism} and J_{AWM}, are determined at the same value of the plastic area, A_{pl}, under the load-displacement curve (see Fig. 1). A reference (solid) line is

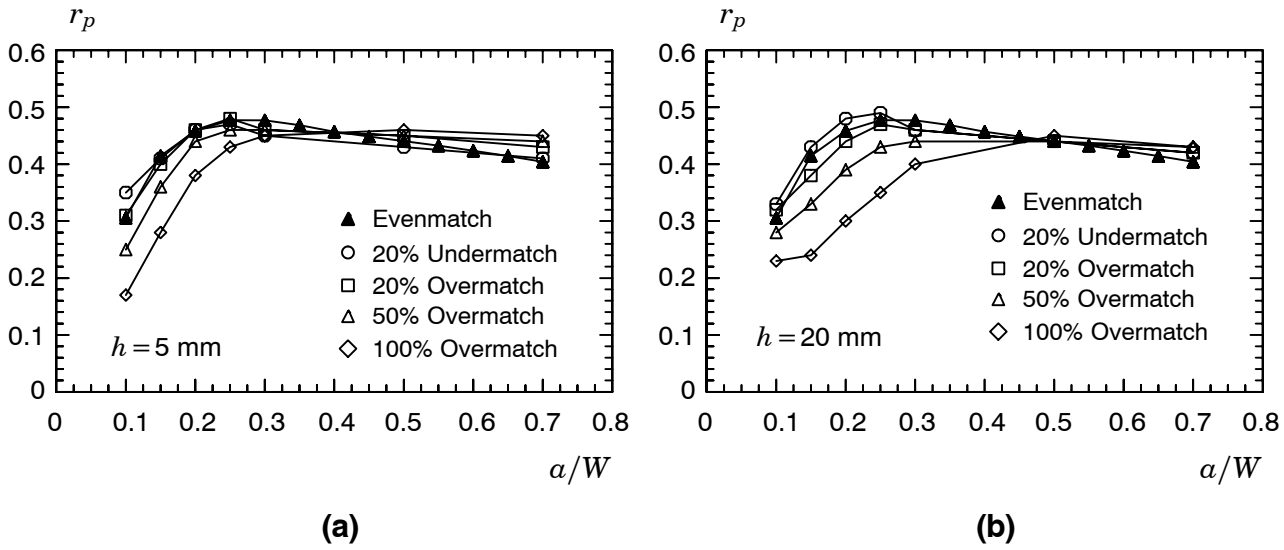

Figure 8 *Variation of plastic rotation factor, r_p, with increased a/W-ratio and different mismatch levels for $h = 5$ and 20 mm groove sizes.*

shown which defines equality between J_{Mism} and J_{AWM}. The results show that J_{Mism}-values increasingly deviate from the corresponding J_{AWM}-values for higher levels of strength mismatch. Consider a 100% mismatch condition: for a given plastic area under the load-displacement curve, the J_{Mism}-value is 30 ~ 40% lower than the corresponding J_{AWM}-value. In contrast, differences between J_{Mism} and J_{AWM} determined at the same A_{pl}-values are within the 10% range for the 20% overmatch condition.

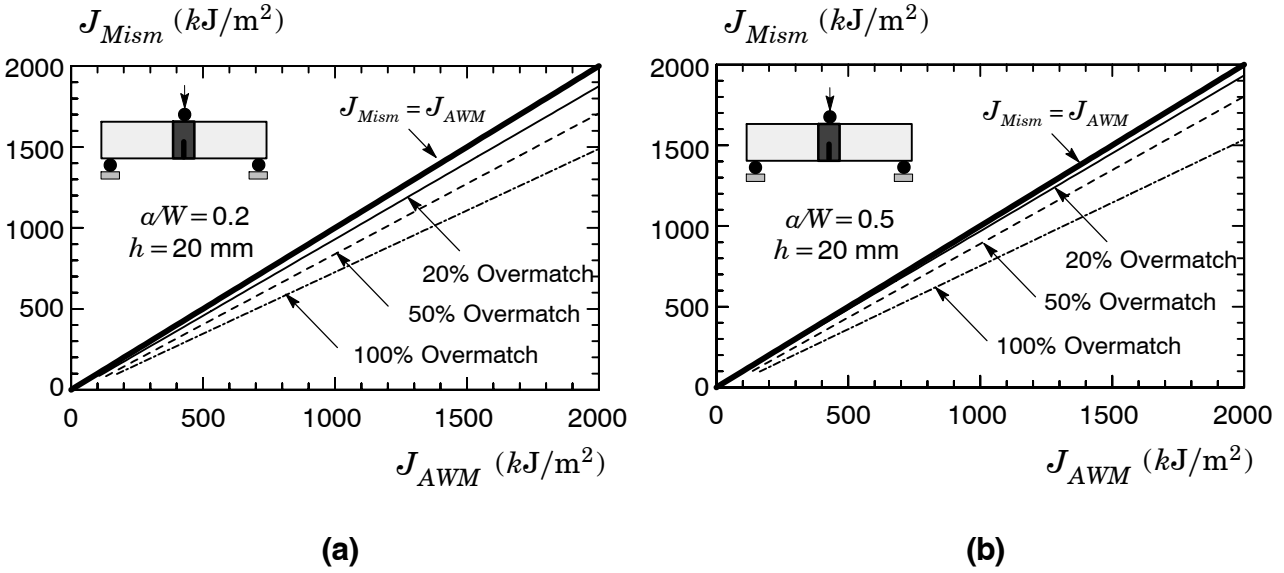

Figure 9 *Comparison of J-values obtained for different overmatch conditions against the corresponding all weld metal condition for deep and shallow crack SE(B) specimens.*

7. CONCLUDING REMARKS

This work addresses the effect of weld strength mismatch on *J* and CTOD estimation formulas which are mainly applicable to determine fracture toughness parameters (J_c or δ_c) from laboratory measurements of load-displacement data using SE(B) fracture specimens. The analyses consider *J* and CTOD estimation procedures for center-cracked, square-grooved bend specimens based upon plastic *eta* factors and plastic rotation factors and include: i) estimating *J* and CTOD from plastic work and ii) estimating CTOD from the plastic rotational factor. The plane-strain results reveal that levels of weld strength mis-

match within the range ± 20% mismatch do not affect significantly *J* and CTOD estimation expressions applicable to homogeneous materials, particularly for deeply cracked fracture specimens. Moreover, CTOD-values derived from using the plastic hinge model display little sensitivity to the mismatch levels as the plastic rotational factor is weakly dependent on strength mismatch, especially for deeply cracked specimens. The present analyses, when taken together with previous studies, provide a fairly extensive body of results which serve to determine parameters *J* and CTOD for different materials using bend specimens with varying geometries and mismatch levels.

8. ACKNOWLEDGMENTS

This investigation is supported by Fundação de Amparo à Pesquisa do Estado de São Paulo (FAPESP) through Grant 03/02735-6 and through a graduate scholarship (04/15719−1) provided to the first author (GHBD).

9. REFERENCES

Anderson, T. L., 2005, *Fracture Mechanics: Fundaments and Applications - 3rd Edition*, CRC Press, New York.

API RP-579, 2000, "Recommended Practice for Fitness-for-Service.", American Petroleum Institute.

ASTM E1290, 1993, "Standard Test Method for Crack-Tip Opening Displacement (CTOD) Fracture Toughness Measurement", American Society for Testing and Materials.

ASTM E1820, 1996, "Standard Test Method for Measurement of Fracture Toughness", American Society for Testing and Materials.

BS 7448, 1991, "Fracture Mechanics Toughness Tests", British Standard.

BS 7910, 1999, "Guide on Methods for Assessing the Acceptability of Flaws in Metallic Structures," British Standard Institution.

Hutchinson, J.W., 1983, ''Fundamentals of the Phenomenological Theory of Nonlinear Fracture Mechanics.'' *Journal of Applied Mechanics*, Vol. 50, pp. 1042-1051.

Koppenhoefer, K., Gullerud, A., Ruggieri, C., Dodds, R. and Healy, B., 1994, ''WARP3D: Dynamic Nonlinear Analysis of Solids Using a Preconditioned Conjugate Gradient Software Architecture." *Structural Research Series (SRS) 596*. UILU-ENG-94-2017. University of Illinois at Urbana-Champaign.

Moran, B., and Shih, C.F., 1987, "A General Treatment of Crack Tip Contour Integrals", *International Journal of Fracture,* Vol. 35, pp. 295−310.

Rice, J. R., Paris, P. C. and Merkle, J. G., 1973, "Some Further Results of *J*-Integral Analysis and Estimates," *Progress in Flaws Growth and Fracture Toughness Testing*, ASTM STP 536, American Society for Testing and Materials, pp 231-245.

Sumpter, J. D. G. and Turner, C. E., 1976, "Method for Laboratory Determination of J_c," *Cracks and Fracture*, ASTM STP 601, American Society for Testing and Materials, pp 3-18.

SINTAP, 1999, "Structural Integrity Assessment Procedure for European Industry". Final Revision. EU-Project BE 95-1462

Zerbst, U., Ainsworth, R. A. and Schwalbe, K.-H., 2000, "Basic Principles of Analytical Flaw Assessment Methods", *International Journal of Pressure Vessels and Piping*, Vol. 77, pp. 855-867.

10. RESPONSIBILITY NOTICE

The authors are the only responsible for the printed material included in this paper.